Evaluation Method of Temperature-Dependent Relaxation Behavior of Polymers

E. Schlosser,* A. Schönhals, H.-E. Carius, and H. Goering

Zentrum für Makromolekulare Chemie, Rudower Chaussee 5, D-12484 Berlin, Germany

Received February 23, 1993; Revised Manuscript Received June 21, 1993•

ABSTRACT: An evaluation technique is proposed which decomposes the temperature-dependent relaxation function of a polymer into the amounts of the overlapping relaxation functions of the individual mechanisms. Each mechanism is described by a seven-parameter model function that is derived from the model function of Havriliak and Negami using temperature-dependent parameters. The evaluation technique is adapted from a method well tried in the frequency domain. For torsional pendulum measurements on a blend of polyamide 6 and ethylene–vinyl acetate copolymer the power of the evaluation method to clear up the morphology is shown.

Introduction

To gain complete information about the number, position, intensity, and shape of the dielectric or mechanical relaxation regions that occur in a polymer, measurements in a broad band of frequencies at different temperatures are required.

As is well known, each relaxation mechanism is indicated by a peak of the loss part and a step of the real part of the complex relaxation function, that is, the permittivity in the case of dielectric spectroscopy or, e.g., shear modulus and shear compliance in the mechanical case. The available information consists in four parameters describing the position of the relaxation process in frequency scale (frequency of loss maximum), the height of the step of the real part (intensity), and the shape of the relaxation function (width and asymmetry).[1]

The maximum frequency is related to the mean relaxation time of the process and characterizes the molecular mobility (at the temperature of investigation), which depends on such parameters as composition, thermal treatment, and mixing with other substances. From an analysis of the intensity information about the fraction of different phases in blends or block copolymers can be obtained, for example. The width and the asymmetry of the relaxation function usually deviate from the values due to the Debye function. Now there is a strong discussion about the physical origin of this deviation,[2,3] but it is known empirically that this effect depends for instance on the degree of cross-linking[4] or microheterogeneity.[5,6]

Because in polymeric solids there exists generally an overlapping of mechanisms, the parameters cannot usually be taken directly from the measured curves. Decomposition of the whole information into the amounts of the individual mechanisms is needed which can be done by a special evaluation method[7] based on model functions.[8,9]

On the other hand, measurements in the temperature domain at constant frequency are widespread. This procedure provides also a loss peak and a step of the real part due to each mechanism. However, the determination of the characteristic parameters is much more difficult than for frequency-dependent measurements, because all parameters change with temperature to some extent. In addition, the shape of the loss curve of each relaxation region depends on the activation energy as a further parameter. Nevertheless, the use of a model function simplifies the evaluation even for an isolated mechanism. Moreover, for overlapping of relaxation regions model functions are necessary for the analysis, as in the frequency domain.

Appropriate model functions with three or four parameters[8,9] have been used for many years both in the frequency domain and in the time domain. In the temperature domain model functions up to now have been used to much less extent and have been mostly discussed with respect to one isolated relaxation region. Read and Williams[10] introduced intensity and position parameters as a function of temperature into the dielectric three-parameter model functions of Kirkwood, Cole–Cole, and Cole–Davidson. Gomez and Calleja[11] discussed the problem of determination of activation energies from $\epsilon''(T)$-measurements using the same model functions with a temperature-dependent position parameter. Havriliak and Watts[12] combined the evaluation of frequency-dependent dielectric data by the four-parameter model function of Havriliak and Negami[13] with the information resulting from data sets obtained at different temperatures.

Alig, Stieber, and Wartewig[14] described the complex ultrasonic longitudinal modulus versus temperature at fixed frequency by the three-parameter Kohlrausch–Williams–Watts function[15] where the mean relaxation time (position parameter) is temperature dependent according to the Vogel–Fulcher relation.[16,17] Almond, Braddell, and Harris used the same model function to represent mechanical absorption spectra close to the glass transition.[18]

Quan, Johnson, Anderson, and Bates applied four Gaussian model fits to analyze the dielectric loss spectrum of 1,4-polybutadiene/1,2-polybutadiene diblock copolymers that exhibit two transitions due to each component.[19]

Recently, Rotter and Ishida[20] employed techniques common to spectroscopy to analyze spectra of tan δ as a function of temperature, obtained by dynamic mechanical measurement at constant frequency (predominantly 1 Hz). The curve-fitting routine that uses a mixture of Gaussian and Lorentzian line shapes is applied to the spectra of different polymers exhibiting one or more relaxation regions.

In this paper we start from the four-parameter model function proposed by Havriliak and Negami[13] in the field of dielectric spectroscopy (frequency domain). By introduction of the temperature dependencies of the relevant parameters an appropriate model function for the complex permittivity in the temperature domain is established, and the evaluation method[7] well tried in the frequency domain is adapted. With some modifications of the model function, the evaluation formalism can be applied also to

• Abstract published in *Advance ACS Abstracts*, October 1, 1993.

0024-9297/93/2226-6027$04.00/0

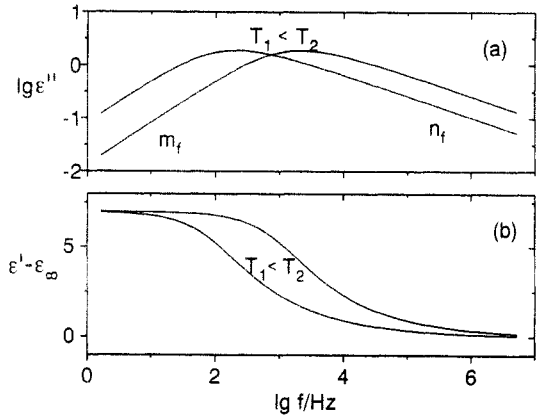

Figure 1. Frequency dependence of the imaginary (a) and real (b) parts of the complex permittivity at two temperatures within a relaxation region.

mechanical measurements. The accuracy of the fit procedure is tested by evaluation of the dielectric permittivity of poly(propylene oxide) determined in the frequency and temperature domains. As an example for the analysis of the temperature-dependent modulus, torsional pendulum measurements on a polymer blend are discussed.

Model Function

A well-known model function that represents the frequency dependence of the complex permittivity $\epsilon^*(f) = \epsilon'(f) - i\epsilon''(f)$ has been introduced by Havriliak and Negami (HN function)[7]

$$\epsilon^*(f) - \epsilon_\infty = \Delta\epsilon[1 + (if/f_c)^\beta]^{-\gamma} \qquad (0 < \beta, \beta\gamma < 1) \quad (1)$$

where

$$\epsilon'(f) - \epsilon_\infty = \Delta\epsilon[r(f)]^{-\gamma} \cos[\gamma\theta(f)] \quad (2)$$

$$\epsilon''(f) = \Delta\epsilon[r(f)]^{-\gamma} \sin[\gamma\theta(f)] \quad (3)$$

with

$$r(f) = [1 + 2(f/f_c)^\beta \cos(\beta\pi/2) + (f/f_c)^{2\beta}]^{1/2} \quad (4)$$

$$\theta(f) = \arctan[\sin(\beta\pi/2)/((f/f_c)^{-\beta} + \cos(\beta\pi/2))] \quad (5)$$

with $i = -1^{1/2}$ and $\epsilon_\infty = \epsilon'(f)$ for $f \gg f_c$. The four parameters concerning the relaxation behavior are $\Delta\epsilon$ (intensity), f_c (characteristic relaxation frequency), and β and γ (shape) which can be found by a least squares fit of $\epsilon''(f)$ and $\epsilon'(f)$ to the data ϵ_i'' and ϵ_i'. Because the real and imaginary parts of the complex permittivity are connected by the Kramers–Kronig relation,[21,22] every one of them provides sufficient information for the fit.

Figure 1 shows the well-known behavior of log ϵ'' (Figure 1a) and ϵ' (Figure 1b) versus log f. The maximum position of the loss curve corresponds with the characteristic frequency f_c for the symmetric shape ($\gamma = 1$) or is near f_c in the asymmetric case. The tails at low and high frequencies ($f \ll f_c, f \gg f_c$) are linear functions with a slope $\partial \log \epsilon''/\partial \log f$ that represents directly the shape parameters $m_f = \beta$ and $n_f = -\beta\gamma$, respectively. For higher temperatures the loss curve is shifted to higher frequencies.

To obtain a model function for the temperature domain $\epsilon^*(T)$, we keep the frequency $f = f_1$ (constant) and should treat all parameters in eq 1 as temperature-dependent (HNT function). However, in good approximation it has been proved sufficient to introduce only the temperature dependence of f_c, which is most prominent, and of $\Delta\epsilon$. The shape parameters β and γ, which hardly change with temperature, are taken as constant.

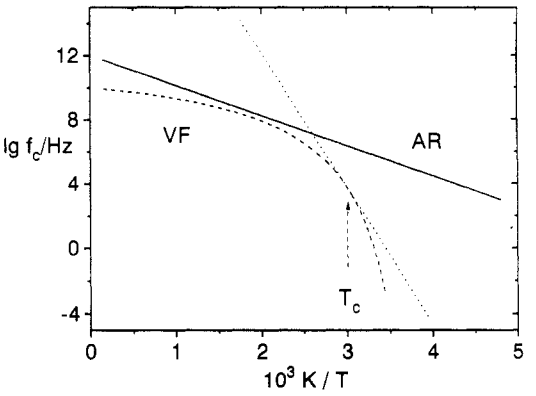

Figure 2. Temperature dependence of the characteristic frequency f_c according to the Arrhenius (full line) and Vogel–Fulcher relations (dashed line, dotted line as approximation).

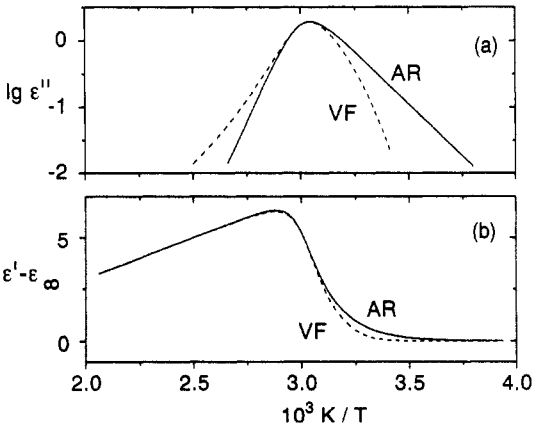

Figure 3. Temperature dependence of the imaginary (a) and real (b) parts of the complex permittivity, with $f_c(T)$ according to the Arrhenius (full line) and Vogel–Fulcher (dashed line) relations.

For a secondary relaxation process (i.e., the β-relaxation in polymers) the temperature dependence of f_c can be described by the Arrhenius-relation (AR)

$$f_c(T) = f_\infty \exp(-\Delta U/RT) \quad (6)$$

with f_∞ the preexponential factor, ΔU the activation energy, and $R = 8.314 \times 10^{-3}$ kJ mol^{-1} K^{-1} (gas constant). The plot of log f_c against $1/T$ (Figure 2, full line) gives a straight line with a slope proportional to the activation energy ΔU.

Introduction of eq 6 into eq 1 leads with $f = f_1$ (frequency of measurement) to a first approximation of the function $\epsilon^*(T)$ for the secondary relaxation regions.

Plots of log ϵ'' and ϵ' versus $1/T$ (Figure 3a,b, full lines) show a maximum and a step, respectively, at (or near) a characteristic temperature T_c that is defined by

$$f_1/f_c(T_c) = 1 \quad (7)$$

T_c is related to the maximum position of $\epsilon''(T)$ analogously to f_c in the frequency domain.

It is appropriate to eliminate log f_∞ in eq 6 and to use T_c. Then the term $f_1/f_c(T)$ in eq 1 can be rewritten as

$$f_1/f_c(T) = \exp[-(\Delta U/R)(1/T - 1/T_c)] \quad (8)$$

It should be noticed that in the temperature domain the tails of the function log $\epsilon''(T)$ are linear versus $1/T$. The slope of the tails for high and low temperature, respectively, is given (as in the frequency domain) by the shape parameters, but they are additionally multiplied by the activation energy ΔU: $m_T = \beta\Delta U$, $n_T = -\beta\gamma\Delta U$.

For $\Delta\epsilon(T)$ we use a linear function versus $1/T$ that may be constant or gradually increase with increasing

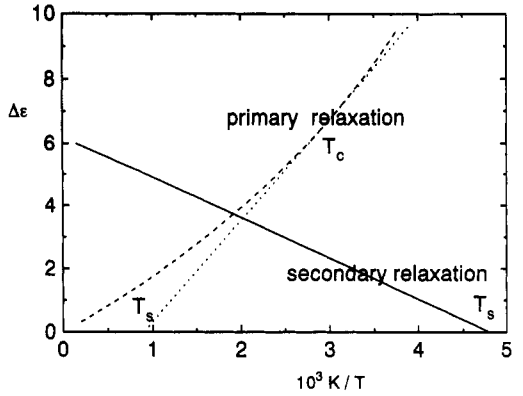

Figure 4. Temperature dependence of the intensity for the secondary (full line) and primary relaxations (dashed line, dotted line as approximation).

temperature[23-25] (Figure 4, full line):

$$\Delta\epsilon(T) = \Delta\epsilon_c(T_c/T)[(T - T_s)/(T_c - T_s)] \quad (T_s < T_c) \quad (9)$$

$\Delta\epsilon_c$ is the intensity at the characteristic temperature T_c. T_s denotes the (extrapolated) temperature for which the intensity becomes zero. For $T_s = 0$ the intensity is independent of the temperature, and for $T_s < T_c$ the intensity increases with increasing temperature (due to the β-process).

Equations 8, 9, and 1 define the final form of the model function for secondary relaxation regions in the temperature domain (HNTAR). The model function contains for each relaxation mechanism six parameters: $\Delta\epsilon_c$ (intensity at T_c), T_c (characteristic temperature), β and γ (same shape parameters as in the frequency domain), ΔU (activation energy of the process), and T_s (characterizing the temperature dependence of the intensity). Contrary to the evaluation in the frequency domain, the additional determination of ΔU and T_s requires also additional information that can normally be gained by involving ϵ_i' data besides the ϵ_i'' data in the fitting procedure.

For complex relaxation processes (like α and normal mode process), $f_c(T)$ is given instead of eq 6 by the Vogel–Fulcher equation[16,17] (VF)

$$f_c(T) = f_\infty \exp(-\Delta U_\infty/R(T - T_0)) \quad (T > T_0) \quad (10)$$

(cf. Figure 2, dashed line), where ΔU_∞ is the activation energy for infinite temperature and T_0 is the Vogel temperature, which is ca. 50 K below the glass transition temperature T_g. Using the characteristic temperature according to eq 7, we get from eq 10

$$f_1/f_c(T) = \exp[-(\Delta U_\infty/R)(1/(T - T_0) - 1/(T_c - T_0))] \quad (11)$$

However, the application of this temperature dependency means that a further (seventh) parameter (T_0) has to be determined for each process. Moreover, this parameter is of second order because it rules the weak curvature of $f_c(T)$ and can be obtained therefore only for very precise data and no strong overlapping with neighboring processes.

Therefore, at strong overlapping of several relaxation regions, some restrictions for the model functions of the α- and β-processes must be introduced to stabilize the fitting procedure. The kind of restriction must be adapted to the special case. An example for that is given in the last section.

Contrary to secondary relaxation, the intensity of the main relaxation increases with temperature. According to the theory of Fröhlich,[26] a linear decrease versus $1/T$ is predicted. Some recent experimental facts[27,28] point to a stronger temperature dependence (cf. dashed line in Figure 4). However, we will restrict ourselves to the linear

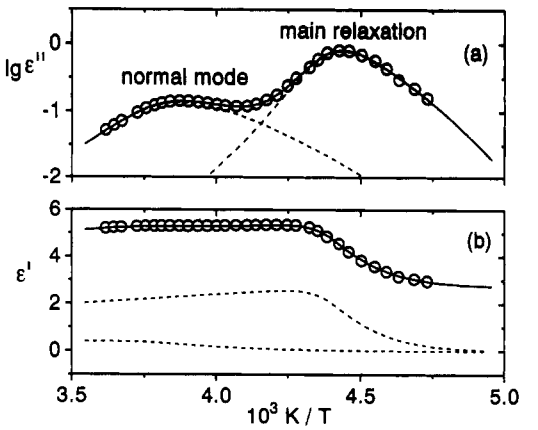

Figure 5. Temperature-dependent dielectric loss (a) and permittivity (b) of poly(propylene oxide) at 10 kHz.

approximation that is formally identical with eq 9, but for $T_s > T_c$ (cf. dotted line in Figure 4).

Thus the temperature-dependent fit function for the main relaxation is given by eqs 1, 9, and 11 (HNTVF).

The application of the HNT function in the field of mechanical measurement, especially to modulus measurement, involves the problem that permittivity is a compliance in the sense of linear response theory, which differs already qualitatively from the mechanical modulus by the frequency dependence of the real part, which increases with increasing frequency. The relation between the complex compliance $J^* = J' - iJ''$ and the complex modulus $G^* = G' + iG''$[29] is given by

$$J^*G^* = 1 \quad (12)$$

Therefore the modulus data can be transformed according to eq 12 by the relations

$$J' = G'/(G'^2 + G''^2) \qquad J'' = G''/(G'^2 + G''^2) \quad (13)$$

into the compliance data before they are analyzed by the HNT function.

Another way is to transform the HN function by eq 12 into the model function for the direct fit of the modulus data (MHN function). This analytical transformation cannot be performed exactly. However, in good approximation a proper model function is given by an expression that differs from the HN function mainly by the reciprocal ratio of frequencies

$$G^*(f) - G_\infty = \Delta G[1 + (-if_c/f)^\beta]^{-\gamma} \quad (14)$$

By splitting eq 14 into real and imaginary parts and by introducing the temperature dependencies of $f_c(T)$ and ΔG according to eqs 8 or 10 and 9, we get the MHNT fit function for the complex modulus.

Test of the Evaluation Method

To test the model function and evaluation method in the temperature domain, we have chosen poly(propylene oxide) of molecular weight 4000 for which the dielectric behavior is known very well from the literature[30,31] and from previous measurements.[32,33] Above the glass transition temperature, besides the main relaxation at higher temperatures, the so-called normal mode process is observed, which is related to the cumulative dipole moment along the contour of the polymer chain.

The complex permittivity has been measured at 1, 2, 4, 10, and 20 kHz in the temperature range 210–260 K. Figure 5 shows the data of ϵ' and ϵ'' versus $1/T$ for $f_1 = 10$ kHz (open circles). The maximum of ϵ'' at higher temperatures is due to the normal mode process and that at lower

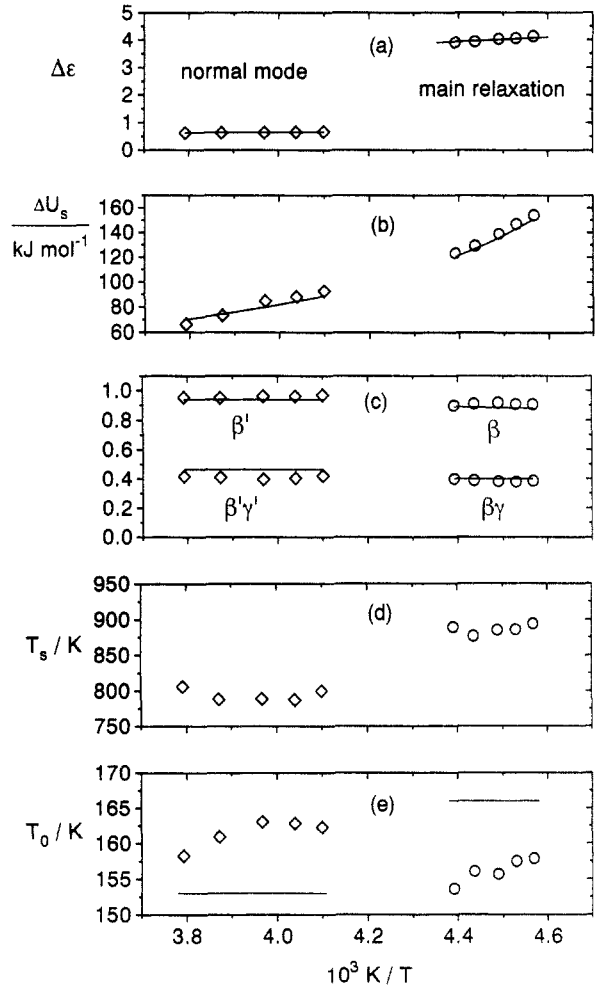

Figure 6. Parameters of normal mode and main relaxation of poly(propylene oxide) versus reciprocical temperature: (a) intensity; (b) apparent activation energy; (c) shape parameters; (d) T_s (due to the temperature dependence of the intensity); (e) Vogel temperature.

temperatures is due to the main relaxation. The mean relaxation times of both relaxation regions are known[32] to shift with temperature according to the Vogel–Fulcher law.[16,17] Therefore, as a fit function the sum of two HNTVF functions is used. The fits to the $\epsilon''(T)$ and $\epsilon'(T)$ data are shown as full lines. The dashed lines are due to the amounts of the individual mechanisms (the amount of ϵ_∞ is omitted for clearness).

In Figure 6 the parameters of the individual mechanisms that were obtained from measurements at five frequencies (open circles) are plotted against the inverse temperature of the maximum position of the loss part. The full lines represent the temperature dependence of the parameters determined in the frequency domain. The correspondence of the intensity $\Delta\epsilon$ (Figure 6a), of the apparent activation energy ΔU_s (Figure 6b), and of the shape parameters β and $\beta\gamma$ (Figure 6c) is of remarkable accuracy for both relaxation regions. The order of magnitude of the fitted T_s values (Figure 6d, $T_s > T_c$) confirms qualitatively the curved temperature dependence of $\Delta\epsilon$ (cf. Figure 4) for the main relaxation as for the normal mode process. However, with $T_0 < T_0'$ (Figure 6e) the Vogel parameters of the two regions show the inverse behavior in comparison with the values derived from measurements in the frequency domain. The reason is not quite clear, but probably it must be ascribed to the uncertainty of the fitting process with respect to these limiting values which are far away from the temperature range of measurement.

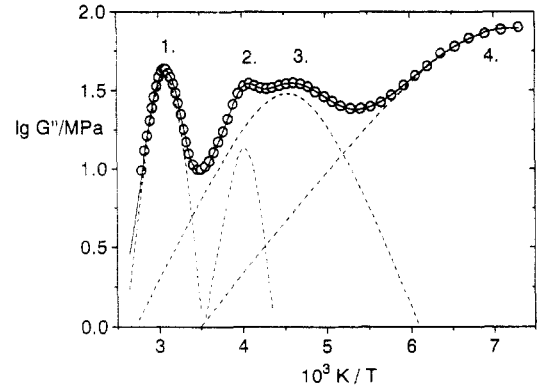

Figure 7. Loss shear modulus of a blend of 70 wt % polyamide 6 (PA6) and 30 wt % ethylene–vinyl acetate (EVA) (open symbols). The solid line is due to the fit function. The dashed lines show the contributions of the individual mechanisms which are involved: (1) α-relaxation of PA6; (2) α-relaxation of EVA; (3) β-relaxation of PA6; (4) other secondary relaxations as γ-relaxation of PA6.

The coincidence of most parameters determined by evaluation in the temperature domain and in the frequency domain justifies subsequently the approximation that the HNT function has been established taking into consideration only the temperature dependence of the HN parameters f_c and $\Delta\epsilon$ and not the shape parameters.

Example for Evaluation of Temperature-Dependent Modulus

Because the structural parameters act in a distinct manner to the different molecular relaxation mechanisms, modulus measurement by the torsional pendulum is a powerful tool to follow chemical and physical changes in polymers if the parameters of the individual relaxation regions can be determined. It will be shown for measurements on a blend of 70 wt % polyamide 6 (PA6) and 30 wt % ethylene–vinyl acetate copolymer (EVA) that, at strong overlapping of the relaxation regions as occurs especially in multicomponent systems, with the aid of the proposed evaluation method, the separation of the regions can be done.

It was the aim of this study to clarify the influence of the thermal treatment on the morphology and the mechanical properties. For comparison, also pure PA6 under the same conditions was measured.

Samples of dimensions 80 × 10 × 4 mm^3 were made by injection molding and stored for 4 weeks at room conditions. Before measurement each sample was annealed at T_a for 1 h and subsequently quenched in liquid nitrogen.

The measurement was performed by a computer-controlled torsional pendulum (ZMC, custom-made). The loss part of the shear modulus of a blend sample that was annealed at 423 K is shown in Figure 7. Four overlapping relaxation regions indicated by $G''(T)$ maxima 1–4 are observed. Their molecular assignment is given in the caption of the figure. Because of the large temperature range and the strong overlapping of all relaxation regions, the following restrictions were made within the frame of evaluation:

(i) Only the imaginary part G'' was fitted.

(ii) The main maxima were fitted taking $f_c(T)$ dependencies according to eq 10 with $\log f_\infty = 10$ (for the α-process of PA6) and $\log f_\infty = 11$ (for the α-process of EVA). With respect to the secondary maxima eq 6 with $\log f_\infty = 14$ was used.

(iii) The temperature dependencies of the intensity were neglected. Among the calculated fit parameters only the

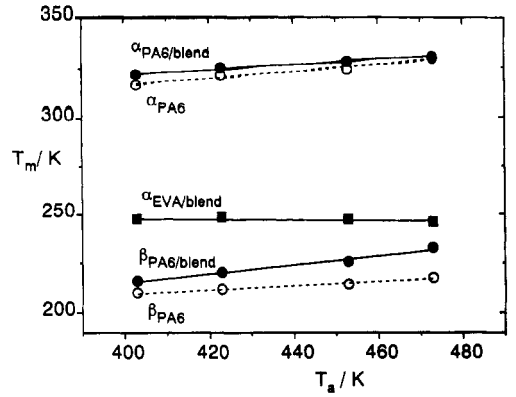

Figure 8. Maximum position of the α- and β-relaxations for different annealing temperatures: (○) pure PA6; (●) PA6 in the blend; (■) EVA in the blend. The dashed and solid lines are only guides for the eyes.

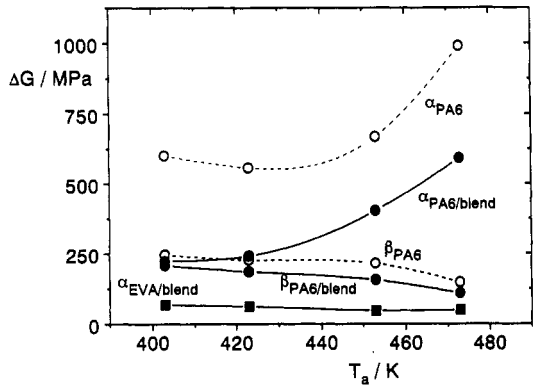

Figure 9. Intensity for the α- and β-relaxations for different annealing temperatures. The lines are only guides for the eyes (symbols as in Figure 8).

temperature of the maximum position T_m and the intensity ΔG versus the annealing temperature T_a for processes 1–3 will be discussed. (The fourth relaxation region was taken into account only within the frame of evaluation because of its influence on the three considered processes.)

According to Figure 8 the maximum temperature T_m of the α- and β-processes of pure PA6 as well as PA6 in the the blend increases with increasing T_a. Due to the well-known hydrophilic behavior of polyamide, the progression of the drying process for higher annealing temperatures can be seen clearly. Because the α-maximum of EVA is not influenced by the moisture content, the water is obviously absorbed only in PA6.

As shown in Figure 9 the intensity of the β-process of PA6 and the PA6 component in the blend (PA6/blend) decreases with increasing T_a. This confirms that water molecules are involved in the β-relaxation. On the contrary, the intensity of the α-process of PA6 and PA6/blend is nearly constant up to annealing temperatures T_a of ca. 400 K but increases dramatically for higher T_a in both materials. Partial melting at annealing temperatures $T_a > 400$ K enhances the fraction of the amorphous phase and therefore also the intensity of the α-process which is related to molecular motion in the amorphous region. The same effect should occur for the β-process, but it is obviously overcompensated by the strong influence of humidity.

Figure 10 shows for the α- and β-processes the ratio Q of the intensity of PA6 in the blend and the value in pure PA6. According to the weight fraction of PA6 in the blend, the intensity should be 70% of the value in pure PA6 for each process. The deviation of the measured values points to a different morphology which is formed during the

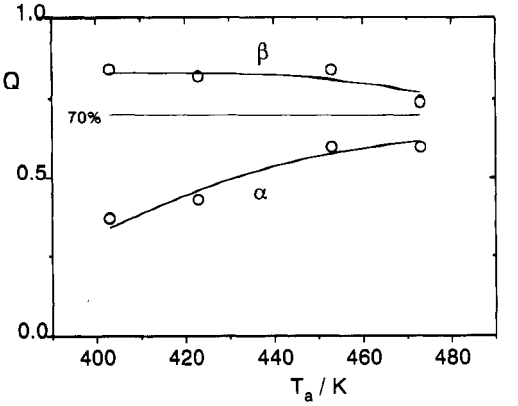

Figure 10. Relative intensity $Q = \Delta G(\text{PA6/blend})/\Delta G(\text{PA6})$ of the α- and β-processes for different annealing temperatures.

injection molding in the amorphous phase of PA6/blend compared with pure PA6. The dispersed EVA particles disturb to some extent the growing of larger and perfect crystallites as formed in pure PA6 and act simultaneously as nuclei for many microcrystallites. In that way within such regions of imperfect crystallization an amorphous phase of restricted mobility is formed as a third phase, which enables only the local β-process but not the large-scale α-relaxation to be active. This phase morphology is not changed by annealing below 400 K, but above 400 K, the imperfect crystallites melt more as T_a increases, reducing the amount of the restricted amorphous phase. Therefore, with increasing T_a, the intensities approach the value corresponding to 70% weight fraction.

With respect to EVA in the blend the independence of the maximum temperature and of the intensity of T_a gives evidence that annealing does not change the interaction between PA6 and EVA. This analysis of torsional pendulum measurements was given to illustrate the power of the proposed evaluation method. A more detailed discussion of the results of the study, especially concerning the properties of the blend, is beyond the scope of this paper and will be published elsewhere.[34]

Acknowledgment. The financial support of the Bundesminister für Forschung und Technologie (Grant 03 M 4053 4) and of the BUNA AG, Schkopau, is gratefully acknowledged. We would like to thank Mr. K. Gruber (BUNA AG) for providing the polymer blends.

References and Notes

(1) Schlosser, E.; Schönhals, A. *Colloid Polym. Sci.* **1989**, *267*, 133.
(2) *Proceedings of the Conference on Relaxations in Complex Systems, Crete, 1990* (Ngai, K. L., Ed.) *J. Non-Cryst. Solids* **1991**, *131*.
(3) Wong, J.; Angell, C. A. *Glass: Structure by Spectroscopy*; Marcel Dekker: New York, 1976.
(4) Bakule, R.; Havranek, A. *Rubber Chem. Technol.* **1978**, *51*, 72.
(5) Fischer, E. W.; Zetsche, A. *Polym. Prepr. (Am. Chem. Soc., Div. Polym. Chem.)* **1992**, *33*, 78.
(6) Roland, C. M.; Ngai, K. L. *Macromolecules* **1992**, *25*, 363.
(7) Schlosser, E.; Schönhals, A. *Colloid Polym. Sci.* **1989**, *267*, 963.
(8) Hill, R. M. *Phys. Stat. Solidi (B)* **1981**, *103*, 319.
(9) Williams, G.; Watts, D. C. *Trans. Faraday Soc.* **1970**, *66*, 80.
(10) Read, B. E.; Williams, G. *Trans. Faraday Soc.* **1961**, *No. 467*, 57; **1979**, Part 11.
(11) Gomez, J. E.; Calleja, R. D. *J. Macromol. Sci., Phys.* **1984**, *B23* (2), 255.
(12) Havriliak, S., Jr.; Watts, D. G. *Polymer* **1986**, *27*, 1509.
(13) Havriliak, S.; Negami, S. *J. Polym. Sci., Polym. Symp.* **1966**, *14*, 99.
(14) Alig, I.; Stieber, F.; Wartewig, S. *Polymer* **1991**, *32*, 2146.
(15) Williams, G.; Watts, D. C. *Trans. Faraday Soc.* **1970**, *66*, 80.

(16) Vogel, H. *Phys. Z.* **1921**, *22*, 645.
(17) Fulcher, G. S. *J. Am. Ceram. Soc.* **1925**, *8*, 339.
(18) Almond, D. P.; Braddell, O. G.; Harris, B. *Polymer* **1992**, *33*, 2234.
(19) Quan, X.; Johnson, G. E.; Anderson, E. W.; Bates, F. S. *Macromolecules* **1989**, *22*, 2451.
(20) Rotter, G.; Ishida, H. *Macromolecules* **1992**, *25*, 2170.
(21) Kronig, R. de L. *J. Opt. Soc. Am.* **1926**, *12*, 547.
(22) Kramers, H. A. *Atti Congr. Fis. Como* **1927**, 545.
(23) Ishida, Y. *Kolloid Z.* **1961**, *174*, 124.
(24) Ishida, Y.; Matsuo, M.; Yamafuji, K. *Kolloid Z.* **1962**, *180*, 108.
(25) Kremer, F.; Hofmann, A.; Fischer, E. W. *Polym. Prepr. (Am. Chem. Soc., Div. Polym. Chem.)* **1992**, *33*, 96.
(26) Fröhlich, H. *Theory of Dielectrics*; Oxford University Press: Oxford, 1949.
(27) Schlosser, E.; Schönhals, A. *Polymer* **1991**, *32*, 2135.
(28) Schönhals, A.; Kremer, F.; Hofmann, A.; Fischer, E. W. *Phys. Rev. Lett.* **1993**, *70*, 3459.
(29) McCrum, N. G.; Read, B. E.; Williams, G. *Anelastic and Dielectric Effects in Polymeric Solids*; Dover: New York, 1991.
(30) Baur, M. E.; Stockmayer, W. H. *J. Chem. Phys.* **1965**, *43*, 4319.
(31) Johari, G. P. *Polymer* **1986**, *27*, 866.
(32) Schlosser, E.; Schönhals, A. *Prog. Colloid Polym. Sci.* **1993**, *91*, 158.
(33) Ngai, K. L.; Schönhals, A.; Schlosser, E. *Macromolecules* **1992**, *25*, 4915.
(34) Carius, H.-E., et al., in preparation.